We would like to thank the editor and all referees for their helpful comment. Based on these comments, we made the following changes to improve the paper:

- Section 1 (Literature review): Two paragraphs were included to explain how previous studies used water level time series or remotely sensed river characteristics such as altimetry or river width for model calibration to put this study and the novelty more into context.
  In response to:
  Editor: "*I do agree that you should definitely add a more comprehensive a state-of-the-art review of the literature presenting approaches that use water levels for calibrating rainfall-runoff models, explaining what differentiate your work from them, in order to justify its publication.*"
  Referee #1: "*Perhaps the proposed paper still present elements of novelty compared to these studies. However, it is the authors' responsibility to illustrate in which terms their analyses complement or advance these previous studies. Is their method new? If not, how does it compare to the methods proposed by Jian et al, 2017? Is it better or worse?*"
- Section 3.4 (Methods, Model calibration): A short explanation including references was added on why the Nash-Sutcliffe function was used.
  In response to:
  Referee #2: "*Section 3.4, page 12. You provide good justification for your use of the water level duration curve as an evaluation metric but still do not provide good justification for why you use the Nash-Sutcliffe Coefficient.* "
- Section 4.5 (Limitations): A paragraph was added on the advantages and disadvantages of the proposed calibration method. This includes limitations as a result of the constant cross-section assumption and additional uncertainties due to adding the slope-roughness parameter of the Strickler-Manning formula as calibration parameter.
  In response to:
  Editor: "*A description of the main features (advantages and disadvantages) of the proposed approach in comparison to the previous literature, may also help in improving the section (4.5) on the Limitations of the work, putting it in the international literature context.*"
  Referee #2: "*Section 4.5, page 19. The limitations are a little brief - these points need expanding alongside some references.*"
  Referee #2: "*I am still not totally convinced by the methodology - in particular the assumption that the cross section does not vary over time and additional uncertainties derived from calibrating additional parameters in the Strickler-Manning formula.*"
- Section 5 (Conclusion) was merged with Section 6 (Recommendations)
  In response to:
  Editor: "*I would suggest merging limitations and recommendations in a single section, dealing with both the limits and way forward.*"
  Referee #2: "*Section 6, page 20. Recommendations are also very brief and don't really warrant their own section - I would move these into your conclusions.*"

Rainfall-runoff modelling using river stage time series in the absence of reliable discharge information: a case study in the semi-arid Mara River Basin

Petra Hulsman[1], Thom A. Bogaard[1], Hubert H.G. Savenije[1]

[1]Water Resources Section, Faculty of Civil Engineering and Geosciences, Delft University of Technology, Stevinweg 1, 2628 CN Delft, the Netherlands

Correspondence to: Petra Hulsman (p.hulsman@tudelft.nl)

Abstract. Hydrological models play an important role in Water Resources Management. These models generally rely on discharge data for calibration. Discharge time series are normally derived from observed water levels by use of a rating curve. However, this method suffers from many uncertainties due to insufficient observations, inadequate rating curve fitting procedures, rating curve extrapolation, and temporal changes in the river geometry. Unfortunately, this problem is prominent in many African river basins. In this study, an alternative calibration method is presented using water level time series instead of discharge, applied to a semi-distributed rainfall runoff model for the semi-arid and poorly gauged Mara River Basin in Kenya. The modelled discharges were converted into water levels using the Strickler-Manning formula. This method produces an additional model output: a "geometric rating curve equation" which relates the modelled discharge to the observed water level using the Strickler-Manning formula and a calibrated slope-roughness parameter. This procedure resulted in good and consistent model results during calibration and validation. The hydrological model was able to reproduce the water levels for the entire basin as well as for the Nyangores sub-catchment in the north. The newly derived geometric rating curves were subsequently compared to the existing rating curves. At the catchment outlet of the Mara, these differed significantly, most likely due to uncertainties in the recorded discharge time series. However, at the 'Nyangores' sub-catchment, the geometric and recorded discharge were almost identical. In conclusion, the results obtained for the Mara river basin illustrate that with the proposed calibration method the water level time series can be simulated well, and that also the discharge-water level relation can be derived, even in catchments with uncertain or lacking rating curve information.

1 Introduction to rating curve uncertainties

Hydrological models play an important role in Water Resources Management. In hydrological modelling, discharge time series are of crucial importance. For example, discharge is used when estimating flood peaks (Di Baldassarre et al., 2012; Kuczera, 1996), calibrating models (Domeneghetti et al., 2012; McMillan et al., 2010) or determining the model structure (Bulygina et al., 2011; McMillan et al., 2015). Discharge is commonly measured indirectly through interpolation of velocity measurements over the cross-section (Di Baldassarre et al., 2009; WMO, 2008). However, to obtain frequent or continues discharge data, this method is time consuming and cost-inefficient. Moreover, in African river catchments, the quantity and quality of the available discharge measurements is unfortunately often inadequate for reliable calibration of hydrological models (Hrachowitz et al., 2013; Shahin, 2002).

There are several sources of uncertainty in discharge data when using rating curves that cannot be neglected. First, measurement errors in the individual discharge measurements affect the estimated continuous discharge data, for example in the velocity-area method uncertainties in the cross-section and velocity can arise due to poor sampling (Pelletier, 1988; Sikorska et al., 2013). Second, these measurements are usually done during normal flows, however during floods the rating curve needs to be extrapolated. Therefore, the uncertainty increases for discharges under extreme conditions (Di Baldassarre et al., 2011; Domeneghetti et al., 2012). Thirdly, the fitting procedure does not always account well for irregularities in the profile, particularly when banks are overtopped. Finally, the river is a dynamic, non-stationary system which influences the rating curve: such as changes in the cross-section due to sedimentation or erosion, backwater effects or hysteresis (Petersen-Øverleir, 2006). The lack of incorporating such temporal changes in the rating curve increases the uncertainty in discharge data (Guerrero et al., 2012; Jalbert et al., 2011; Morlot et al., 2014). As a result, the rating curve should be regularly updated to take such changes into account. The timing of adjusting the rating curve relative to the changes in the river affects the number of rating curves and the uncertainty (Tomkins, 2014). Previous studies focused on assessing the uncertainty of rating curves (Clarke, 1999; Di Baldassarre et al., 2009) and their effect on model predictions (Karamuz et al., 2016; Sellami et al., 2013; Thyer et al., 2011).

In the Previous studies focused on assessing the uncertainty of rating curves (Clarke, 1999; Di Baldassarre et al., 2009) and their effect on model predictions (Karamuz et al., 2016; Sellami et al., 2013; Thyer et al., 2011). However, in the absence of reliable rating curves, remotely sensed river characteristics related to the discharge data, such as river width and water level time seriescan provide reliable and valuable information on the flow dynamics (Seibert et al., 2016) and therefore could be a good alternative for model calibration and validation. For instance, previous studies derived the discharge from remotely sensed river width (Revilla-Romero et al., 2015; Sun et al., 2015; Yan et al., 2015) or river water levels measured with radar altimetry (Michailovsky et al., 2012; Pereira-Cardenal et al., 2011; Ričko et al., 2012; Schwatke et al., 2015; Sun et al., 2012; Tourian et al., 2017). Radar altimetry observations of river water levels were also used to calibrate or validate hydrological models using empirical equations transforming discharge to water level without using cross-section information (Getirana, 2010; Sun et al., 2012). Moreover, hydrological models were calibrated on river width or surface water extent (Revilla-Romero et al., 2015; Sun et al., 2015).

Besides remotely sensed river characteristics, also locally measured river water level time series are valuable for model calibration. and validation. In general, water levels time series are more reliable

3

than discharge data or remotely sensed river characteristics as these are direct measurements and not processed data. However, the potentialIn previous studies, river water level time series were used for model calibration using the Spearman rank correlation coefficient (Jian et al., 2017; Seibert et al., 2016) or by including an inverse rating curve with three new calibration parameters to convert the modelled discharge to water level (Jian et al., 2017). When using the Spearman rank correlation function, the focus is on correlating the ranks instead of calibrating models the magnitudes, which as a result introduces biases in the model results. Alternatively, rainfall-runoff models can be calibrated on water level time series has not been studied in detail, especially in combinationcombined with a hydraulic equation, and in poorly gauged semi-arid areas introducing only one new calibration parameter.

The goal of this study is to illustrate the potential of water level time series for model calibration by incorporating a hydraulic equation describing the rating curve within the model. This calibration method is applied to the semi-arid and poorly gauged Mara River Basin in Kenya. For three gauging stations within this basin, the quality of the recorded rating curves have been analysed and compared to the model results. For this purpose, a semi-distributed rainfall runoff model has been developed on a daily timescale applying the FLEX-Topo modelling concept (Savenije, 2010).

2 Site description of the Mara River Basin and data availability

The Mara River originates in Kenya in the Mau Escarpment and flows through the Masai Mara National Reserve in Kenya into Lake Victoria in Tanzania. The main tributaries are the Nyangores and Amala Rivers in the upper reach and the Lemek, Talak and Sand in the middle reach (Figure 1). The first two tributaries are perennial while the remaining tributaries are ephemeral, which generally dry out during dry periods. In total, the river is 395 km long (Dessu et al., 2014) and its catchment covers an area of about 11,500 km^2 (McClain et al., 2013) of which 65% is located in Kenya (Mati et al., 2008).

Within the Mara River Basin, there are two wet seasons linked to the annual oscillations of the ITCZ (Inter-tropical Convergence Zone). The first wet season is from March to May and the second from October to December (McClain et al., 2013). The precipitation varies spatially over the catchment following the local topography. The largest annual rainfall can be found in the upstream area of the catchment: between 1000 and 1750 mm/yr. In the middle and downstream areas, the annual rainfall is between 900 and 1000 mm/yr and between 300 and 850 mm/yr, respectively (Dessu et al., 2014).

The elevation of the river basin varies between 3000 m above sea level at the Mau Escarpment, 1480 m at the border to Tanzania and 1130 m at Lake Victoria (McClain et al., 2013). In the Mara River Basin, the main land cover types are agriculture, grass, shrubs and forests. The main forest in the catchment is the Mau Forest, which is located in the north. Croplands are mainly found in the north and in the south, whereas the middle part is dominated by grasslands.

2.1 Data availability

2.1.1 In situ monitoring data

In the Mara River Basin, long term daily water level and discharge time series are available for 44-60 years between 1955 and 2015 at the downstream station near Mines and in the two main tributaries: the Nyangores and Amala. In addition, precipitation and air temperature is measured at 27 and 7 stations, respectively (Figure 1 and Table 1). However, the temporal coverage of these data is poor as there are many gaps.

There are many uncertainties in the discharge and precipitation data in the Mara River Basin. Discharge data analyses indicated that the time series were unreliable due to various inconsistencies in the data, especially at Mines and Amala. At Mines, a high scatter in the discharge-water level graph was observed (Figure 2); also back-calculated cross-section average flow velocities were below 1 m/s (Figure S1) whereas in 2012 the measured velocity was 2.13 m/s and discharge 529.3 m^3/s (GLOWS-FIU, 2012). At Amala, the rating curves were adjusted multiple times affecting mostly the low flows. Only the rating curve at Nyangores was stable and consistent with field measurements. The precipitation data analysis showed a high spatial variability between the limited number of rainfall stations available. More information can be found in the supplement "S1 Data quality".

During field trips, point discharge measurements were done in September/October 2014 at Emarti Bridge, Serena Pump House and New Mara Bridge, see Table 2 and Figure 3. At each location, the discharge was derived using an Acoustic Doppler Profiler (Sontek RiverSurveyor M9) mounted on a portable raft which is also equipped with a Power Communications Module and a DGPS antenna (Rey et al., 2015).
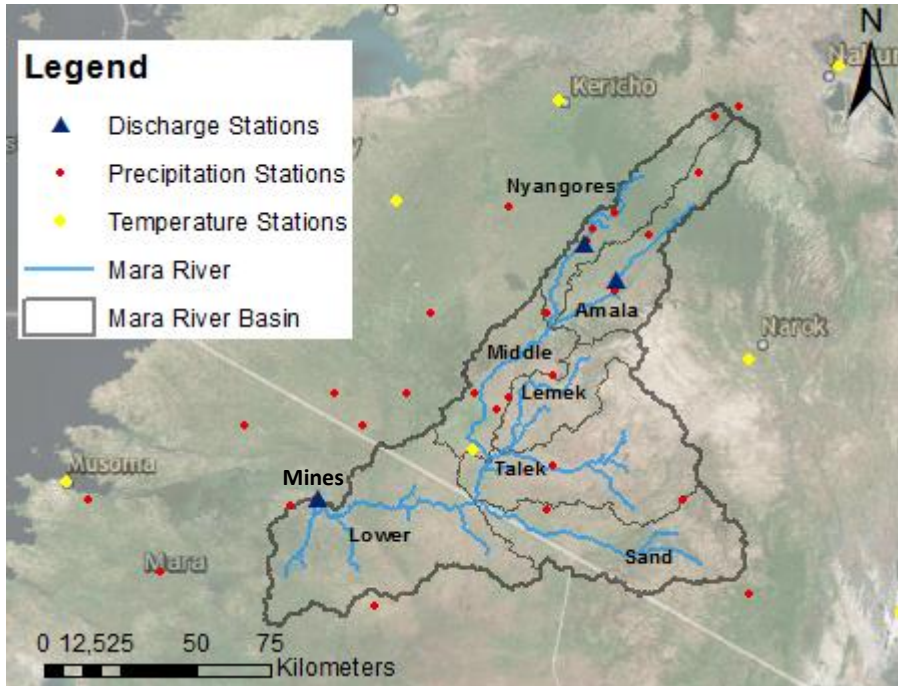
Figure 1: Map of the Mara River Basin and the hydro-meteorological stations for which data is available
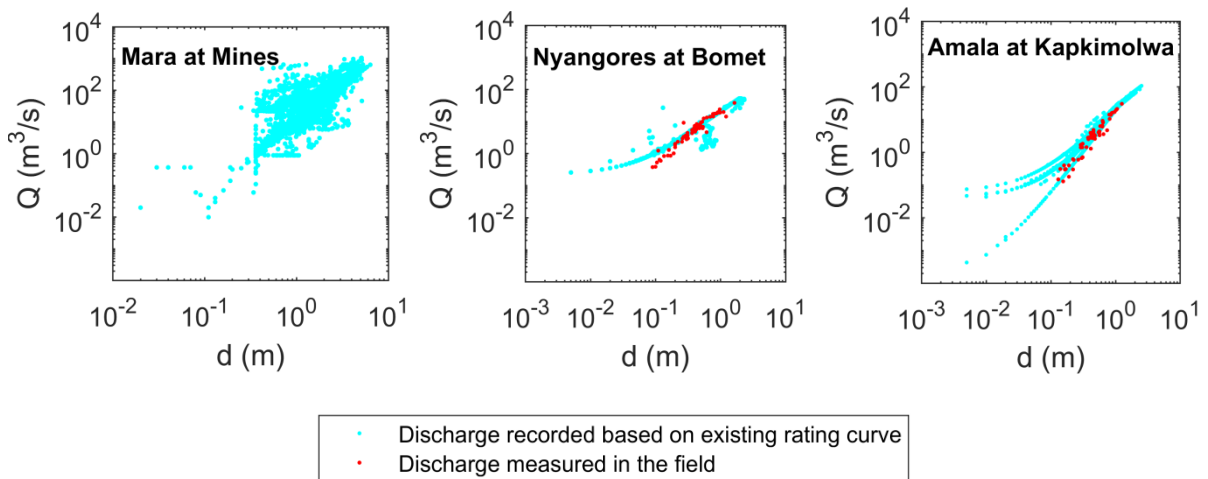

Figure 2: Discharge - water depth graphs for the three main river gauging stations in the Mara River Basin: Mara at Mines, Nyangores at Bomet and Amala at Kapkimolwa. 1) Recorded discharge and water level time series between 1960 and 2010 (light blue), 2) discharge field measurements from the Nile Decision Support Tool (NDST) for the time period 1963 - 1989 (Nyangores) and 1965 - 1992 (Amala), no data was available for Mines (red)

Table 1: Hydro-meteorological data availability in the Mara River Basin. The temporal coverage for water level and discharge can be different due to poor administration.

	Precipitation	Temperature	Water level, discharge		
Number of stations	28	7		3	
Station ID	-	-	1LA03	1LB02	5H2
Station location	-	-	Nyangores at Bomet	Amala at Kapkimolwa	Mara at Mines
Time range	1959 -2011	1957 - 2014	1963-2009	1955-2015	1969-2013
Duration [years]	0 - 43	3 - 57	46	60	44
Coverage	8 - 100%	30 -100%	Discharge: 85% Water level: 85%	Discharge: 72% Water level: 70%	Discharge: 53% Water level: 61%

Table 2: Discharge measured in the field using an Acoustic Doppler Profiler (Sontek RiverSurveyor M9) mounted on a portable raft which is also equipped with a Power Communications Module and a DGPS (Rey et al., 2015)

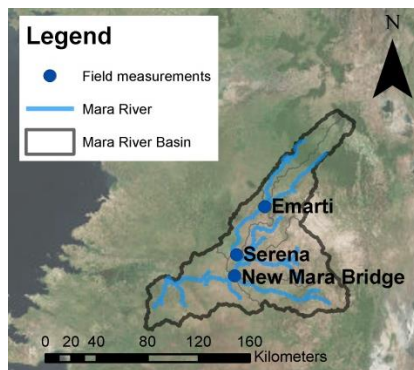| Station name	Date	Mean discharge	Standard deviation
Emarti Bridge	13 Sep 2014	19.2 m^3/s	0.7 m^3/s
	4 Oct 2014	13.4 m^3/s	0.6 m^3/s
Serena Pump House	9 Oct 2014	16.6 m^3/s	0.4 m^3/s
New Mara Bridge	19 Sep 2014	19.6 m^3/s	0.6 m^3/s
	6 Oct 2014	21.9 m^3/s	0.4 m^3/s

Figure 3: Map of discharge measurement locations during field trips in September/October 2014

2.1.2 Remotely sensed data

Besides ground observations, also remotely sensed data were used for setting up the rainfall-runoff model. Catchment classification was based on topography and land cover. For the topography, a digital elevation map (SRTM) with a resolution of 90 m and vertical accuracy of 16 m was used (U.S. Geological Survey, 2014). The land cover was based on Africover, a land cover database based on ground truth and satellite images (FAO, 1998). For the climate, remotely sensed precipitation was used from FEWSNET on a daily timescale from 2001 to 2010 and monthly actual evaporation from USGS from 2001 to 2013. Moreover, NDVI maps derived from Landsat images were used to define parameter constraints.

3 Hydrological model setup for the Mara River Basin

3.1 Catchment classification based on landscape and land use

For this study, the modelling concept of FLEX-Topo has been used (Savenije, 2010). It is a semi-distributed rainfall runoff modelling framework that distinguishes hydrological response units (HRUs) based on landscape features. The landscape classes were identified based on the topographical indices HAND (Height Above Nearest Drain) and slope using a digital elevation map. Hillslopes are defined by a strong slope and high HAND, wetlands by a low HAND, and terraces by a high HAND and mild slope. The threshold for the slope (21.9%) was based on a sensitivity analyses within the Mara Basin which revealed that the area of a hillslopes changed asymptotically with the threshold. Therefore, the slope threshold was chosen at the point where changes in the sloped area become insignificant. As the wetland area was insignificant based on field observations, the HAND threshold was set to zero. In the Mara River Basin, there are mainly terraces and hillslopes.

To further delimit these two main landscape units, the land cover is taken into account as well. In the upper sub-catchments, there are mainly croplands and forests, whereas further south the land use is dominated by grasslands. In the lower sub-catchment, there are mostly croplands and grasslands. This resulted in four HRUs within the sub-basin of the Mara River Basin: forested hillslopes, shrubs on hillslopes, agriculture and grassland (Figure 4, Figure 5 and Table 3).

Table 3: Classification results: area percentage of each hydrological response unit per sub-catchment in the Mara River Basin

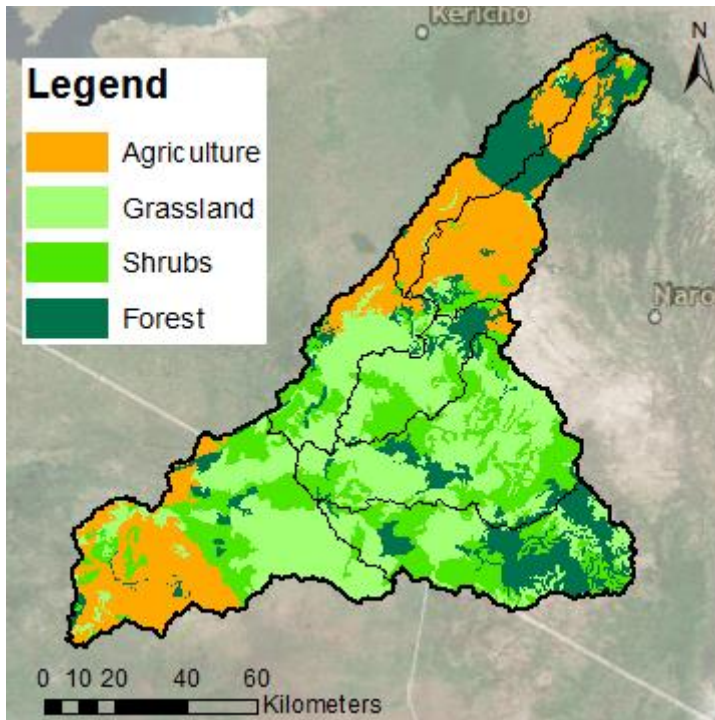| Sub-catchment	Agriculture	Shrubs on hillslopes	Grassland	Forested hillslopes
Amala	67%	0%	0%	33%
Nyangores	61%	0%	0%	39%
Middle	19%	16%	65%	0%
Lemek	10%	39%	51%	0%
Talek	0%	21%	79%	0%
Sand	0%	42%	58%	0%
Lower	26%	23%	52%	0%

Figure 4: Classification of the Mara River Basin into four hydrological response units for each sub-catchment based on land use and landscape

3.2 Hydrological model structure

Each HRU is represented by a lumped conceptual model; the model structure is based on the dominant flow processes observed during field trips or deducted from interviews with local people. For example, in forests and shrub lands, Shallow Subsurface Flow (SSF) was seen to be the dominating flow mechanism: Rainwater infiltrates into the soil and flows through preferential flow paths to the river. In contrast, grassland and cropland generate overland flow. The observed soil compaction, due to cattle trampling and ploughing, reduces the preferential infiltration capacity resulting in overland flow during heavy rainfall. Consequently, there Hortonian Overland Flow (HOF) occurs at high rainfall intensities excessing the maximum infiltration capacity. The perception of the dominant flow mechanisms (Figure 5) was then used to develop the model structure (Figure 6). This approach of translating a perceptual model into a model concept (Beven, 2012) was applied successfully in previous FLEX-Topo applications (Gao et al., 2014a; Gharari et al., 2014).

The model structure contains multiple storage components schematised as reservoirs (Figure 6). For each reservoir, the inflow, outflow and storage are defined by water balance equations, see Table 4. Process equations determine the fluxes between these reservoirs as a function of input drivers and their storage. HRUs function in parallel and independently from each other. However, they are connected through the groundwater system and the drainage network. To find the total runoff at the sub-catchment outlet $Q_{m,sub}$, the outflow $Q_{m,i}$ of each HRU is multiplied by its relative area and then added up together with the groundwater discharge Q_s. The relative area is the area of a specific HRU divided by the entire sub-catchment area. Subsequently, the modelled discharge at the catchment outlet is obtained by using a simple river routing technique where a delay from sub-catchment outlet to catchment outlet was added assuming an average river flow velocity of 0.5 m/s. In the Sand sub-

catchment, it is schematised that runoff can percolate to the groundwater from the river bed and that moisture can evaporate from the groundwater through deep rooting or riparian vegetation.

Table 4: Equations applied in the hydrological model. The formulas for the unsaturated zone are written for the hydrological response units: *Forested hillslopes* and *Shrubs on hillslopes*; for grass and agriculture, the inflow P_e changes to Q_F. The modelling time step is $\Delta t = 1$ day. Note that at a time daily step, the transfer of interception storage between consecutive days is assumed to be negligible.

| Reservoir system	Water balance equation	Process functions
Interception	$\frac{\Delta S_i}{\Delta t} = P - P_e - E_i \approx 0$	$E_i = \min\left(E_p, \min(P, I_{max})\right)$
Surface	$\frac{\Delta S_o}{\Delta t} = P_e - Q_F - Q_{HOF} - E_o$	$Q_F = \min(\frac{S_o}{\Delta t}, F_{max})$
		$Q_{HOF} = \max\frac{(0, S_o - S_{max})}{\Delta t}$
		$E_o = \max(0, \min\left(E_p - E_i, \frac{S_o}{\Delta t}\right))$
Unsaturated zone	$\frac{\Delta S_u}{\Delta t} = (1 - C) * P_e - E$	$C = 1 - \left(1 - \frac{S_u}{S_{u,max}}\right)^{\beta}$
		$E = \min((E_p - E_i), \min\left(\frac{S_u}{\Delta t}, (E_p - E_i) * \frac{S_u}{S_{u,max}} * \frac{1}{C_e}\right))$
Groundwater recharge		$R_s = W * C * P_e$
Fast runoff	$\frac{\Delta S_f}{\Delta t} = R_{fl} - Q_f$	$R_{fl} = T_{lag}(C * P_e - R_s)$ → in a linear delay function T_{lag}
		$Q_f = \frac{S_f}{K_f}$
Groundwater	$\frac{\Delta S_s}{\Delta t} = R_{s,tot} - Q_s - E_s + Q_{inf}$	$R_{s,tot} = \sum_{i=1}^{i=4} R_{s;HRU_i}$
		$Q_s = \frac{S_s}{K_s}$
		$E_s = 0$ and $Q_{inf} = 0$ for all sub − basins except Sand
		$Q_{inf} = \min\left(\frac{S_{s,max} - S_s}{\Delta t}, Q_f\right)$ for Sand sub − basin
		$E_s = \max\left(0, \min\left(E_p - E_i - E_o - E, \frac{S_s}{\Delta t}\right)\right)$ for Sand sub − basin
Total runoff		$Q_m = Q_s + \sum_{i=1}^{i=4} Q_{f;HRU_i}$
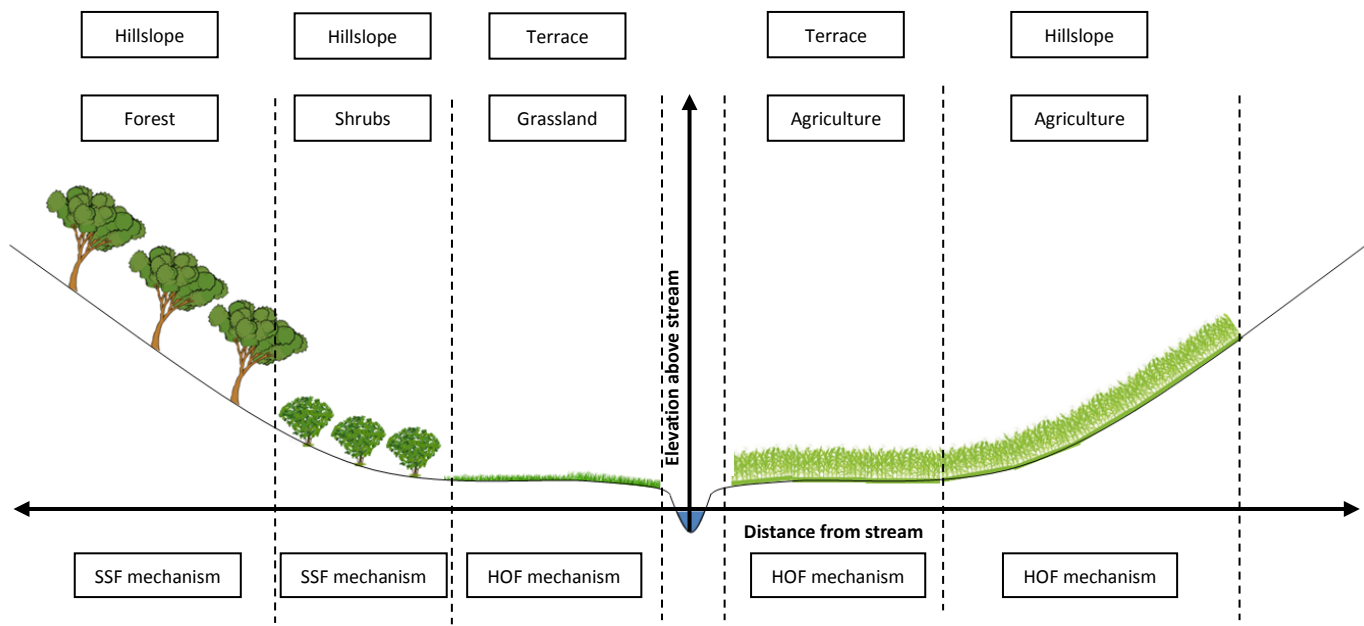
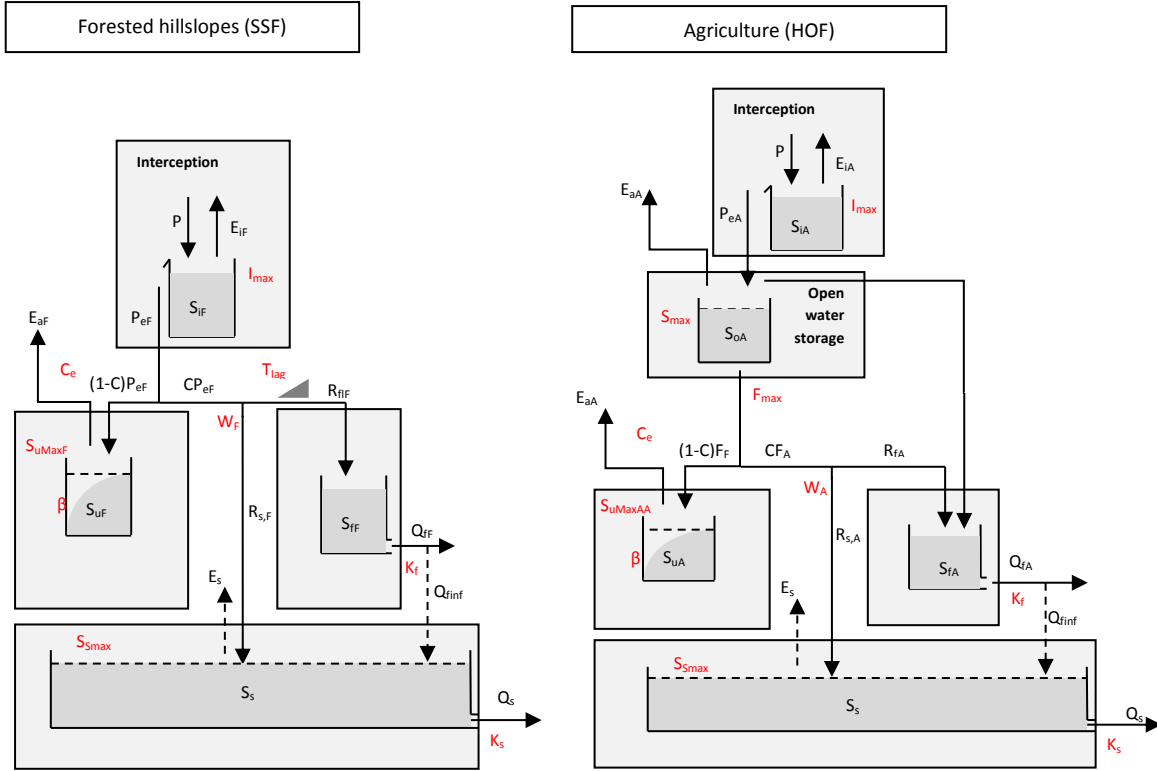**Figure 5: Schematization of the landscape and land use based classification**

| Forested hillslopes (SSF) | Agriculture (HOF) |

Figure 6: Model structure of the HRUs: *Forested hillslopes* **(left) and** *Agriculture* **(right). The structure for** *Shrubs on hillslopes* **is similar to the left one replacing the indices F with S. The structure for** *Grassland* **is similar to the right one replacing the indices A with G. Parameters are marked in red, storages and fluxed in black. Symbol explanation:** <u>Fluxes:</u> precipitation (*P*), evaporation of the interception zone (*E_i*), actual evaporation (*E_a*), evaporation from groundwater only applied in the sub-catchment Sand (*E_s*), effective precipitation (*P_e*), infiltration into the unsaturated zone (*F_A*), discharge from unsaturated zone to the fast runoff zone (*R_f*), groundwater recharge (*R_s*), discharge from the fast runoff (*Q_f*), infiltration into groundwater system only applied in the sub-catchment Sand (Q_f, inf), discharge from the slow runoff (*Q_s*). <u>Storages:</u> storage in the interception zone (*S_i*), open water storage (*S_oA*), storage in the root zone (*S_u*), storage for the slow runoff (S_s), storage for the fast runoff (*S_f*). <u>Remaining symbols:</u> splitter (*W*), splitter (*C*), soil moisture distribution coefficient (*β*), transpiration coefficient (*C_e* = 0.5), reservoir coefficient (*K*); indices f and s indicate the fast and slow runoff. <u>Units:</u> fluxes [mm/d], storages [mm], reservoir coefficient [d], remaining parameters [-].

3.3 Model constraints

Parameters and process constraints were applied to eliminate unrealistic parameter combinations and constrain the flow volume. Parameter constraints were applied to the maximum interception, reservoir coefficients, the storage capacity in the root zone or on the surface, and the slope-roughness parameter, Table 5. Process constraints were applied to the runoff coefficient, groundwater recharge, interception and infiltration, Table 6. The effect of including these parameter and process constraints is illustrated in Figure S5. For instance, the maximum storage in the unsaturated zone $S_{u,max}$ equals the root zone storage capacity and was estimated using the method of Gao (2014) based on remotely sensed precipitation and evaporation (Gao et al., 2014b; Wang-Erlandsson et al., 2016). The dry season evaporation has been derived from the actual evaporation using the NDVI.

Table 5: Overview of all parameter constraints applied in the hydrological model for the Mara River Basin

Parameter	Symbol	Formula	Comment
Interception	I_{max}	$I_{max,forest} > I_{max,grass}, I_{max,shrubs},$	Based on perception

		$I_{max,cropland}$	
		$I_{max,shrubs} > I_{max,grass}, I_{max,cropland}$	
Reservoir coefficient	K_s, K_f	$K_s > K_f$	Based on perception
Storage capacity in unsaturated zone	$S_{u, max}$	$S_{R,y_i} = \int P_e - E_d\, dt$	Based on NDVI, equivalent to the root zone storage capacity (Gao et al., 2014b)
		With: $\frac{E_d}{E_a} = \frac{\text{NDVI}_D}{\text{NDVI}_A}$ thus: $E_d = E_a * \frac{\text{NDVI}_D}{\text{NDVI}_A}$	$S_{R, yi}$: required storage for year i P_e: effective rainfall over dry season E_d: annual mean dry season evaporation, calculated assuming a linear relation between the evaporation and the NDVI E_a: actual mean annual evaporation NDVI_D: annual mean dry season NDVI NDVI_A: annual mean actual NDVI Through a statistical analysis of S_R using the Gumbel distribution, the storage capacity $S_{u, max}$ with a return period of 20 years is calculated.
Reservoir coefficient for groundwater system	K_s	$Q_s = Q_{t=0} * exp\left(-\frac{t}{K_s}\right)$	Based on hydrograph recession analysis Q_s: groundwater discharge
Maximum surface water storage	S_{max}	-	Based on DEM assuming S_{max} is equal to the sink volumes
Slope-roughness parameter	c	$Q = c * A * R^{\frac{2}{3}} = u * A$ $u = c * R^{\frac{2}{3}} \rightarrow c_{calculated} = \frac{u}{R^{\frac{2}{3}}}$ $c_{calculated,-25\% error} < c < c_{calculated,+25\% error}$	Based on Strickler formula, cross-section data and a single discharge and velocity measurement at Mines allowing a wide error margin of 25%

Table 6: Overview of all process constraints applied in the hydrological model for the Mara River Basin

Process	Symbol	Formula	Comment
Average annual runoff coefficient	C	$C = 1 - \dfrac{E}{P} = e^{-\frac{E_p}{P}}$	Based on the Budyko curve using the 95% percentile, hence the modelled average annual runoff coefficient should be below the 95-percentile of the observations
Groundwater recharge	R_s	$R_{s,F} > R_{s,C},\ R_{s,G}$	Based on the assumption that deeper rooting vegetation creates preferential drainage patterns
Annual interception	E_i	$E_{i,F} > E_{i,G},\ E_{i,S}$	Based on the assumption that the interception is higher in forests than in grassland and shrublands
Fast runoff infiltration	-	$f_{Q_{river}} < 3\ \mathrm{yr}^{-1}$	Frequency of river runoff. Based on interviews, locals seldom observed runoff more than 3 times a year.

3.4 Model calibration method using water levels

The hydrological model was calibrated on a daily timescale applying the MOSCEM-UA algorithm (Vrugt et al., 2003) with parameter ranges and values as indicated in Table S1 and S2. For the calibration, the Nash-Sutcliffe coefficient was calculated on(Nash et al., 1970) was applied to the water level duration curve (Eq.1 linear, and Eq.2 log-scale). This frequently used objective function is advantageous as it is sensitive to high flows, but also to low flows when using logarithmic values (Krause et al., 2005; McCuen Richard et al., 2006; Pushpalatha et al., 2012). By calibrating on the duration curve, the focus is on the flow statistics and not on the timing of individual flow peaks. This information is also in the time series. This is justified since there were high uncertainties in the timings of floods events due to the limited number of available rainfall stations to capture the spatial variability of the rainfall input well. Therefore, duration curves were considered as a good signature for calibrating this model; this was also concluded in previous studies (Westerberg et al., 2011; Yadav et al., 2007).

$$\mathrm{NS_d} = 1 - \frac{\Sigma(h_{mod,sorted} - h_{obs,sorted})}{\Sigma(h_{obs,sorted} - h_{obs,avg})} \tag{1}$$

$$\mathrm{NS_{log(d)}} = 1 - \frac{\Sigma(\log(h_{mod,sorted}) - \log(h_{obs,sorted}))}{\Sigma(\log(h_{obs,sorted}) - \log(h_{obs,avg}))} \tag{2}$$

For the water level based calibration, the modelled discharge needs to be converted to modelled water level. This calculation was done with the Strickler-Manning formula in which the discharge is a function of the water level (Eq. (3)), where R is the hydraulic radius (Eq. (6)), A the cross-sectional area (Eq. (5)), i the slope, k the roughness and c the slope-roughness parameter (Eq. (4)). The hydraulic radius and cross-section are a function of the water depth d which is the water level subtracted h by the reference level h_0 (Eq. (7)). The cross-sections were simplified as a trapezium with river width B and two different river bank slopes i_1 and i_2; these coefficients (Table 7) were estimated based on the available cross-section information (Figures S6 – S8). Since the slope and roughness are unknown, the slope-roughness parameter c was calibrated.

$$Q = k * i^{\frac{1}{2}} * A * R^{\frac{2}{3}} = c * A * R^{\frac{2}{3}} \tag{3}$$

$$c = k * i^{\frac{1}{2}} \tag{4}$$

$$A = B * d + \frac{1}{2} * d * (i_1 + i_2) * d \tag{5}$$

$$R = \frac{A}{B + d * \left((1+i_1^2)^{\frac{1}{2}} + (1+i_2^2)^{\frac{1}{2}} \right)} \tag{6}$$

$$d = h - h_0 \tag{7}$$

Table 7: Coefficients used for the river cross-section

	River width B [m]	River bank slope i_1 [-]	River bank slope i_2 [-]	Reference level h_0 [m]
Amala	10.0	3.50	1.83	0
Nyangores	19.05	2.65	5.56	0
Mines	43.81	3.53	3.66	10

This model calibration method, illustrated graphically in Figure 7, was applied to three basins individually: the entire river basin using the station Mines, and for the sub-catchments Nyangores and Amala. At each location, the model was calibrated and validated for time periods indicated in Table 8; at Mines two time periods were used for validation to maximise the use of the available ground measurements.

Table 8: Time periods used for the calibration and validation at three basins: Mines, Nyangores and Amala

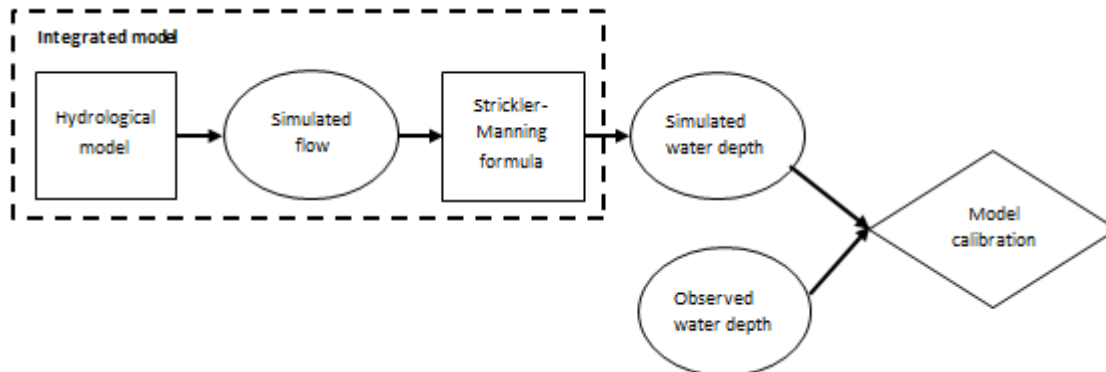|	Mines	Nyangores	Amala
Calibration time period	1970-1974	1970-1980	1991-1992
Validation time period	1980-1981	1981-1992	1985-1986
	1982-1983		

Figure 7: Flow chart of the proposed calibration method

3.5 Rating curve analysis

After calibration, the modelled water levels and discharges were analysed. For the model calibration and validation, the modelled and recorded water levels were compared at basin level, focusing on the time series and the duration curves. Hereafter, water level – discharge relations were analysed taking two rating curves into consideration:

- "Recorded rating curve", relating Q_{rec} to h_{obs},
- "Geometric rating curve", relating $Q_{Strickler}$ to h_{obs}.

The geometric rating curve relates the modelled discharge $Q_{Strickler}$ to the observed water level h_{obs}. This discharge $Q_{Strickler}$ was calculated with the Strickler-Manning formula using the calibrated slope-roughness parameter c, cross-section data, and the observed water level $h_{obs.}$ Therefore, the equation behind the geometric rating curve basically is the Strickler-Manning formula (Eq. (3)) instead of the traditional rating curve equation (Eq. (8)). The advantage of the Strickler-Manning formula is that only one parameter is unknown (river bed slope and roughness c, Eq. (4)), instead of two (fitting parameters a, and b). However, the Strickler-Manning rating curve approach requires additional information on the cross-section.

$$Q = a * (h - h_0)^b \tag{8}$$

4 Results and discussion

4.1 Water level time series and duration curve

Model results were analysed graphically (Figure 8 to Figure 10 and Figure S9 to Figure S19) and numerically based on the Nash-Sutcliffe values for the objective functions (Table 9). The results of the objective functions indicate that at Nyangores and Mines the calibration and validation results were consistent. At Mines, the modelled water level was simulated well, particularly with regard to the duration curve (Figure 8). At individual events, there were substantial differences. In some years, for example in 1974, the observed data were very well represented by the model outcome, however, in other years this was not the case. In general, the model captured the dynamics in the water level well. This was the case during both calibration and validation (see Figure S12 and S13).

At Nyangores the observed and modelled water levels were also similar during calibration and validation, extreme high flows excluded (Figure 9). However, at Amala, the observed and modelled water levels differed significantly during calibration (Figure 10) and validation (Figure S15). The model missed several discharge events completely, likely related to missing rain fall events in the input data due to the high heterogeneity in precipitation.

Table 9: Overview of the values of the objective functions for each model simulation. Calibration was done based on the water level: $NS_{log(h)}$ and NS_h; for comparison, objective functions using the discharge were added here as well

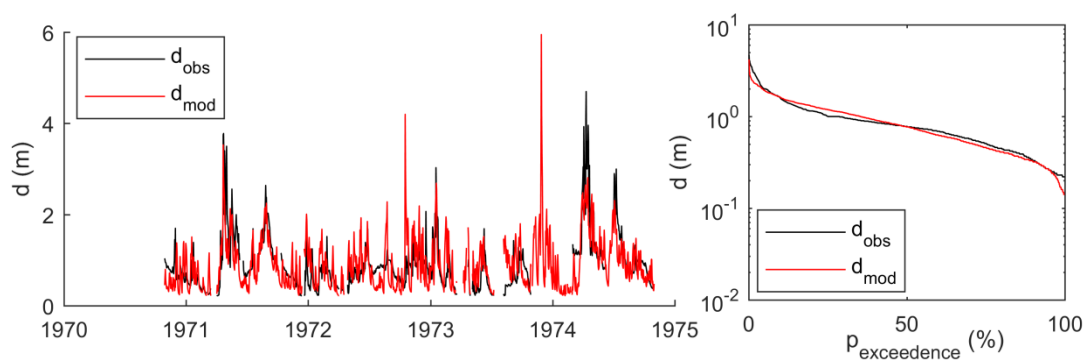|	Nyangores		Amala		Mines		
	Calibration	Validation	Calibration	Validation	Calibration	Validation 1	Validation 2
$NS_{log(d)}$	0.92	0.75	0.92	-0.23	0.97	0.81	0.93
NS_d	0.80	0.69	0.26	0.37	0.97	0.92	0.89
$NS_{log(Q)}$	0.92	0.69	0.57	0.63	0.97	0.81	0.93
NS_Q	0.55	0.37	0.08	-1.67	0.90	0.76	0.77

Figure 8: Model results at Mines during calibration: water depth time series and water depth exceedance
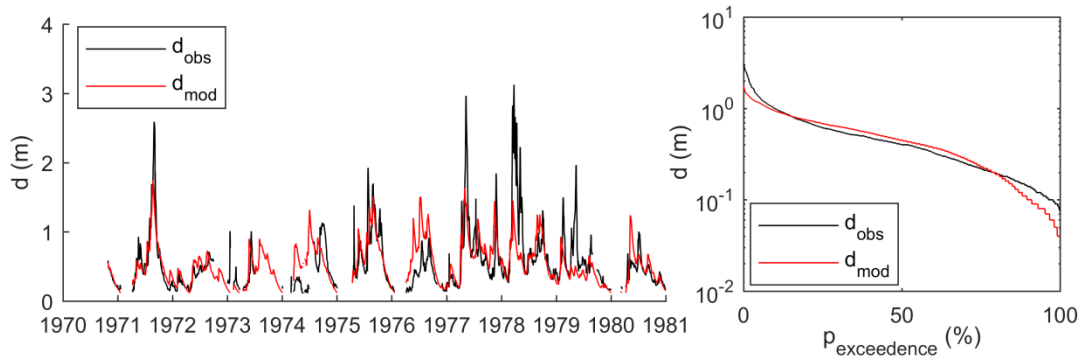
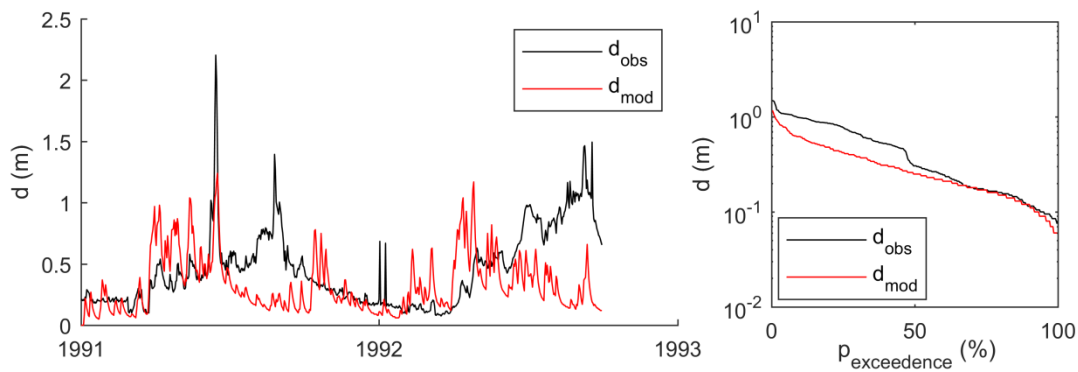**Figure 9: Model results at Nyangores during calibration: water depth time series and water depth exceedance**

Figure 10: Model results at Amala during calibration: water depth time series and water depth exceedance

4.2 Discharge at sub-catchment level

At Mines, the discharge originates from seven different sub-catchments, each with a different contribution. Based on field observations, the mountainous upstream sub-catchments from the north should have the largest contribution whereas the contribution from the relatively drier and flatter Lemek and Talek tributaries from the eastern part of the catchment should be relatively low. The contribution of each sub-catchment to the total modelled discharge was assessed on a monthly timescale and compared with observations.

As shown in Figure 11, the contribution varied throughout the year. In the summer (July-September), the modelled discharge mainly originates from the northern sub-catchments, Nyangores and Amala. However, in the winter (November-April), the modelled discharge mainly originates from the Sand and Lower sub-catchments. The eastern Middle, Talek and Lemek sub-catchments have the lowest discharge throughout the entire year just as observed.
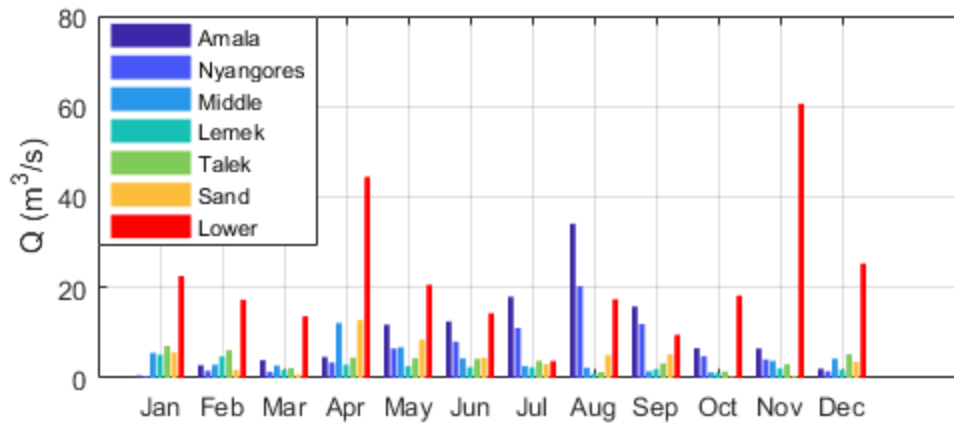
Figure 11: Monthly averaged modelled discharge for each sub-catchment

In previous studies, it has been shown that only a few discharge measurements can contain sufficient information to constrain model predictive uncertainties effectively (Seibert et al., 2009). To evaluate the model at sub-catchment level, model results were compared with discharge measurements done during field trips in September/October 2014 at Emarti Bridge, Serena Pump House and New Mara Bridge. At all three locations, the point measurements fitted well within the range of the modelled discharge (see Figure 12).
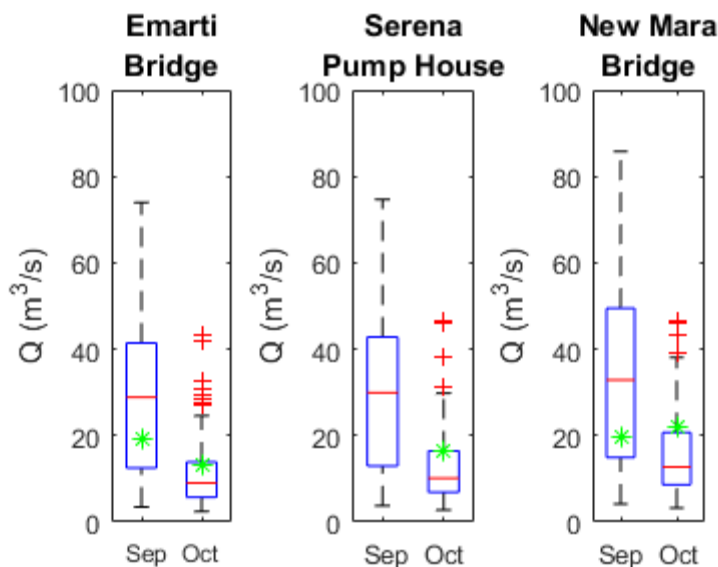

Figure 12: Boxplot of the modelled discharge at three locations; the green asterix represents the measured discharge in Sep/Oct 2014

4.3 Rating curve analysis

In this study, the recorded and geometric (Strickler-Manning) rating curves were compared (Figure 13). At Mines, these two rating curves differed significantly. For medium to high flows, both rating curves, recorded and geometric, run parallel indicating similar cross-sectional properties; only the off-set differed through changing river bed levels. On the other hand, the simulated cross-section average flow velocity were realistic compared to the point measurements at Mines indicating that velocities are greater than 2 m/s during high flows (see Figure 13). At Nyangores, the recorded and geometric rating curves were almost identical, while there were significant differences at Amala

19

gauging station, especially in the low flows. Interestingly, these observations also hold for the validation period for all three stations.

The difference between the recorded and geometric rating curves at Mines probably resulted from uncertainties in the available recorded discharge data. In the complete discharge – water level graphs for all available data (Figure S2), large scatter was found. This could be the result of natural variability in the reference water level h_0 in the rating curve equation which was not taken into account. A sensitivity analysis of the recorded rating curve equation at Mines showed that a deviation of 0.1 m in the reference water level could alter the discharge with 4% for high flows and 46% for low flows. However, a deviation of 0.5 m resulted in a 19% – 325% change in the discharge. Therefore, unnoticed variations in the river bed level strongly affects the uncertainty in the recorded rating curve at Mara Mines, which is located in morphologically dynamic section of the river (Stoop, 2017).

At Amala, the difference between both rating curves could be related to the effect of missing rain events in the input data as result of the short time series for calibration and validation. This resulted in absent discharge peaks and hence an underestimation of the flow; most extremely at Amala. During model calibration, this was compensated by increasing the parameter c in the Strickler-Manning formula (Eq. (4)). As a result, discharge values during missed events were increased, but also for all other days. The compensation effect was limited though since the model was calibrated on the duration curves instead of the time series. As parameter c is linearly related to the geometric rating curve (Eq. (3)), the latter was overestimated as well. Therefore, missing rain events in the input data resulted in the overestimation of the geometric rating curve.

In short, at the two stations with inconsistent rating curves, Amala and Mines, the geometric rating curve deviated significantly from the recordings. Strikingly, the deviations were observed at the same flow magnitudes where large inconsistencies were found in the observations, for instance in the low flows at Amala. However, at the gauging station with a reliable rating curve, Nyangores, the geometric and recorded discharge-water level relations were almost identical.
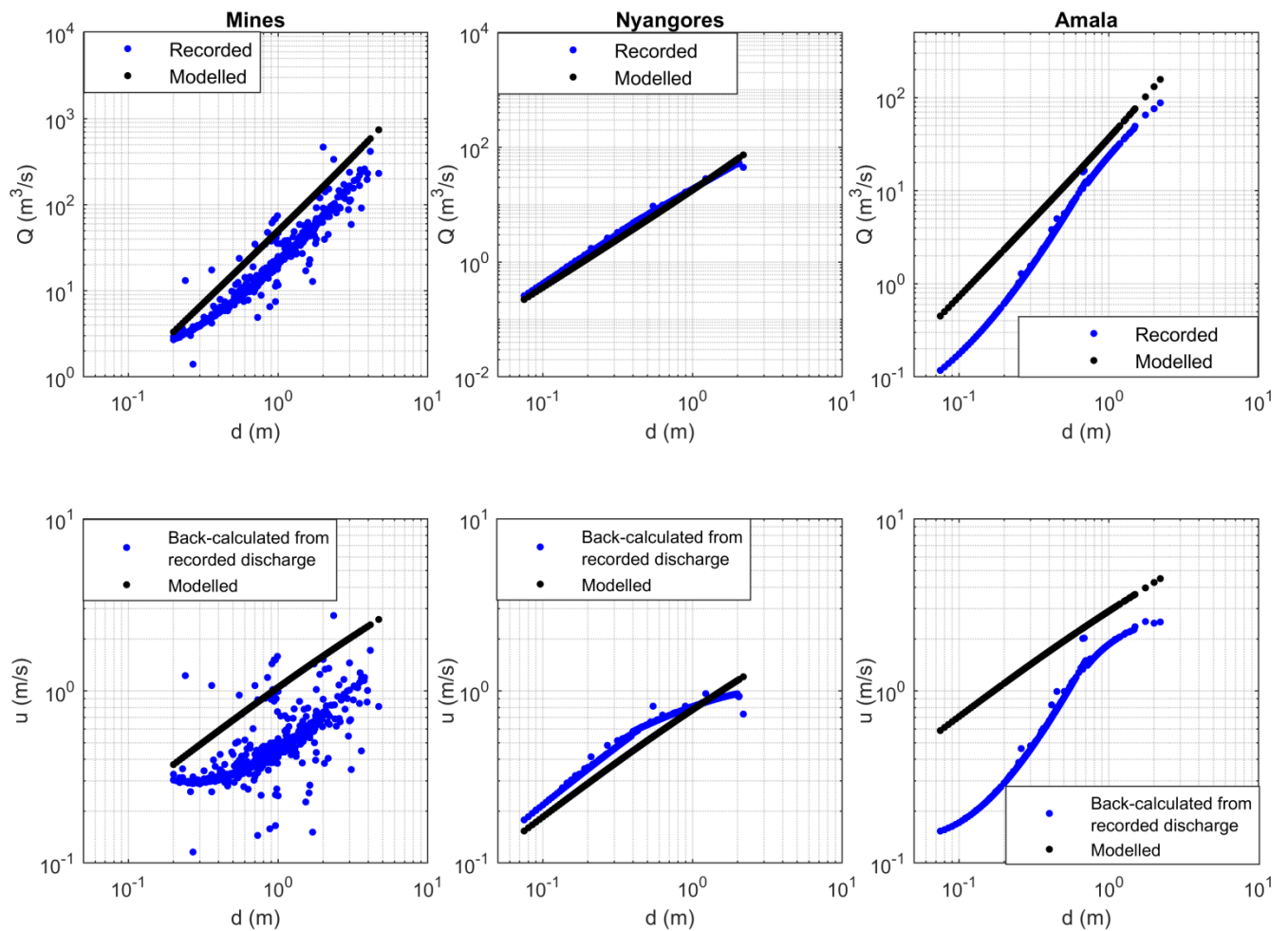
Figure 13: Model calibration results at Mines, Nyangores and Amala: Discharge – water depth graphs (upper) and velocity – water depth graphs (lower).

4.5 Limitations

~~This study illustrates the potential of water level time series for model calibration, also in semi-arid river basins with insufficient discharge data.~~ This paper illustrated that the proposed water level calibration method simulated the discharge-water level relation well for the gauging station where consistent rating curve information was available. However, there are several limitations to this method. First, the slope-roughness parameter compensates for non-closure effects in the water balance, for instance due to errors in the precipitation which is extremely heterogeneous in semi-arid Mara basin. Unfortunately, this heterogeneity is poorly described in our study area with the available rain gauges (see section S7.2 on the precipitation data analysis) influencing the modelling results. Therefore, this parameter should be constrained to minimize this compensation as much as possible. Second, the cross-section was assumed to be constant during the modelling time period. Data analyses indicated that expected changes in the river width or slope cannot affect the rating curve significantly. However, if this is not the case, then this cross-section change should be included during the model calibration.

Previous studies analysed alternative calibration methods by relating the discharge to river characteristics such as river width or water level, for instance using remote sensing data (Revilla-Romero et al., 2015; Schwatke et al., 2015; Yan et al., 2015). River water level time series were used

for model calibration by using the Spearman rank correlation function (Seibert et al., 2016) or an inverse rating curve to convert the modelled discharge to water level (Jian et al., 2017). Compared to these approaches, the calibration method proposed in this paper has the following advantages: 1) water level time series are direct measurements and therefore more reliable compared to processed data such as satellite based measurements, 2) merely one new calibration parameter (the slope-roughness parameter) is introduced instead of three when using an inverse rating curve, and 3) the model is calibrated on water level magnitudes instead of only the ranks which would introduce biases. However, this method also has several disadvantages: 1) cross-section information is needed and is assumed to be constant over the time period for which it is applied, and 2) the newly introduced slope-roughness parameter compensates for non-closure effects in the water balance when not constrained well.

5 Summary and Conclusion

The goal of this paper was to illustrate a new calibration method using water level time series instead of discharge in a semi-arid and poorly gauged basin. This method offers a potential alternative for calibration on discharge data, as is common practice also in poorly gauged catchments. The semi-distributed rainfall runoff modelling framework FLEX-Topo was applied. The catchment was divided into four hydrological response units (HRUs) and seven sub-catchments based on the river tributaries. For each HRU, a unique model structure was defined based on the observed dominant flow processes. By constraining the parameters and processes, unrealistic parameter sets were excluded from the calibration parameter set and the flow volume was constrained. This model was calibrated based on water levels to capture the flow dynamics. For this purpose, the modelled discharge was converted to water levels using the Strickler-Manning formula. The unknown slope-roughness parameter was calibrated.

An important output of this calibration approach is the "geometric rating curve equation" which relates the discharge to the water level using the Strickler-Manning formula. The geometric and recorded rating curves were significantly different at the following two gauging stations: Mines, the catchment outlet, and Amala, a sub-catchment outlet. At both locations, the deviations were with the same flow magnitudes where large inconsistencies were found in the observations. However, at the gauging station with a reliable rating curve, Nyangores, the recorded and geometric discharge-water level relations were almost identical. In conclusion, this calibration method allows reliable simulations of the discharge-water level relation, even in a data poor region.

In addition, this paper analysed the current status of the hydro-meteorological network in the Mara River Basin focusing on the data availability and quality. Moreover, a hydrological model and an improved geometric rating curve equation were developed for this river. All three aspects contribute to improving the assessment of the water resources availability in the Mara River Basin.

6 Recommendations

For future studies, it~~This paper illustrated that the proposed water level calibration method simulated the discharge-water level relation well for the gauging station where consistent rating curve information was available. It~~ would be interesting to apply this calibration method to other

study river basins with different climatic conditions and better data availability. Furthermore, it is recommended to assess the effect of rainfall uncertainties on this calibration method. Moreover, the hydrological model was calibrated on two signatures and two objective functions only. However, it has not been analysed whether these signatures and objective functions provide sufficient information for calibration. Therefore, the procedures for water level based calibration should be analysed in more detail.

Acknowledgement

References

Beven, K. J. (2012). Rainfall-runoff modelling : the primer. Retrieved from http://public.eblib.com/choice/publicfullrecord.aspx?p=822562

Bulygina, N., & Gupta, H. (2011). Correcting the mathematical structure of a hydrological model via Bayesian data assimilation. *Water Resources Research, 47*(5), n/a-n/a. doi:10.1029/2010WR009614

Clarke, R. T. (1999). Uncertainty in the estimation of mean annual flood due to rating-curve indefinition. *Journal of Hydrology, 222*(1-4), 185-190. doi:10.1016/S0022-1694(99)00097-9

Dessu, S. B., Melesse, A. M., Bhat, M. G., & McClain, M. E. (2014). Assessment of water resources availability and demand in the Mara River Basin. *CATENA, 115*(0), 104-114. doi:http://dx.doi.org/10.1016/j.catena.2013.11.017

Di Baldassarre, G., & Claps, P. (2011). A hydraulic study on the applicability of flood rating curves. *Hydrology Research, 42*(1), 10-19. doi:10.2166/nh.2010.098

Di Baldassarre, G., Laio, F., & Montanari, A. (2012). Effect of observation errors on the uncertainty of design floods. *Physics and Chemistry of the Earth, Parts A/B/C, 42–44*, 85-90. doi:http://dx.doi.org/10.1016/j.pce.2011.05.001

Di Baldassarre, G., & Montanari, A. (2009). Uncertainty in river discharge observations: a quantitative analysis. *Hydrol. Earth Syst. Sci., 13*(6), 913-921. doi:10.5194/hess-13-913-2009

Domeneghetti, A., Castellarin, A., & Brath, A. (2012). Assessing rating-curve uncertainty and its effects on hydraulic model calibration. *Hydrology and Earth System Sciences, 16*(4), 1191-1202. doi:10.5194/hess-16-1191-2012

Gao, H., Hrachowitz, M., Fenicia, F., Gharari, S., & Savenije, H. H. G. (2014a). Testing the realism of a topography-driven model (FLEX-Topo) in the nested catchments of the Upper Heihe, China. *Hydrol. Earth Syst. Sci., 18*(5), 1895-1915. doi:10.5194/hess-18-1895-2014

Gao, H., Hrachowitz, M., Schymanski, S. J., Fenicia, F., Sriwongsitanon, N., & Savenije, H. H. G. (2014b). Climate controls how ecosystems size the root zone storage capacity at catchment scale. *Geophysical Research Letters, 41*(22), 2014GL061668. doi:10.1002/2014GL061668

Getirana, A. C. V. (2010). Integrating spatial altimetry data into the automatic calibration of hydrological models. *Journal of Hydrology, 387*(3–4), 244-255. doi:http://dx.doi.org/10.1016/j.jhydrol.2010.04.013

Gharari, S., Hrachowitz, M., Fenicia, F., Gao, H., & Savenije, H. H. G. (2014). Using expert knowledge to increase realism in environmental system models can dramatically reduce the need for calibration. *Hydrol. Earth Syst. Sci., 18*(12), 4839-4859. doi:10.5194/hess-18-4839-2014

GLOWS-FIU. (2012). Environmental Flow Recommendation for the Mara River, Kenya and Tanzania: Global Water for Sustainability program (GLOWS). Miami, FL.

Guerrero, J. L., Westerberg, I. K., Halldin, S., Xu, C. Y., & Lundin, L. C. (2012). Temporal variability in stage-discharge relationships. *Journal of Hydrology, 446-447*, 90-102. doi:10.1016/j.jhydrol.2012.04.031

Hrachowitz, M., Savenije, H. H. G., Blöschl, G., McDonnell, J. J., Sivapalan, M., Pomeroy, J. W., Arheimer, B., Blume, T., Clark, M. P., Ehret, U., Fenicia, F., et al. (2013). A decade of Predictions in Ungauged Basins (PUB)—a review. *Hydrological Sciences Journal, 58*(6), 1198-1255. doi:10.1080/02626667.2013.803183

Jalbert, J., Mathevet, T., & Favre, A. C. (2011). Temporal uncertainty estimation of discharges from rating curves using a variographic analysis. *Journal of Hydrology, 397*(1-2), 83-92. doi:10.1016/j.jhydrol.2010.11.031

Jian, J., Ryu, D., Costelloe, J. F., & Su, C.-H. (2017). Towards hydrological model calibration using river level measurements. *Journal of Hydrology: Regional Studies, 10*, 95-109. doi:https://doi.org/10.1016/j.ejrh.2016.12.085

Karamuz, E., Osuch, M., & Romanowicz, R. J. (2016) The influence of rating curve uncertainty on flow conditions in the River Vistula in Warsaw. *Vol. none. GeoPlanet: Earth and Planetary Sciences* (pp. 153-166).

Krause, P., Boyle, D. P., & Bäse, F. (2005). Comparison of different efficiency criteria for hydrological model assessment. *Advances in Geosciences, 5*, 89-97. doi:10.5194/adgeo-5-89-2005

Kuczera, G. (1996). Correlated rating curve error in flood frequency inference. *Water Resources Research, 32*(7), 2119-2127. doi:10.1029/96WR00804

Mati, B. M., Mutie, S., Gadain, H., Home, P., & Mtalo, F. (2008). Impacts of land-use/cover changes on the hydrology of the transboundary Mara River, Kenya/Tanzania. *Lakes & Reservoirs: Research and Management, 13*(2), 169-177.

McClain, M. E., Subalusky, A. L., Anderson, E. P., Dessu, S. B., Melesse, A. M., Ndomba, P. M., Mtamba, J. O. D., Tamatamah, R. A., & Mligo, C. (2013). Comparing flow regime, channel hydraulics and biological communities to infer flow-ecology relationships in the Mara River of Kenya and Tanzania. *Hydrological Sciences Journal, 59 (3-4)*, 1-19. doi:10.1080/02626667.2013.853121

McCuen Richard, H., Knight, Z., & Cutter, A. G. (2006). Evaluation of the Nash–Sutcliffe Efficiency Index. *Journal of Hydrologic Engineering, 11*(6), 597-602. doi:10.1061/(ASCE)1084-0699(2006)11:6(597)

McMillan, H., Freer, J., Pappenberger, F., Krueger, T., & Clark, M. (2010). Impacts of uncertain river flow data on rainfall-runoff model calibration and discharge predictions. *Hydrological Processes, 24*(10), 1270-1284. doi:10.1002/hyp.7587

McMillan, H. K., & Westerberg, I. K. (2015). Rating curve estimation under epistemic uncertainty. *Hydrological Processes, 29*(7), 1873-1882. doi:10.1002/hyp.10419

Menne, M. J., Durre, I., Korzeniewski, B., McNeal, S., Thomas, K., Yin, X., Anthony, S., Ray, R., Vose, R. S., Gleason, B. E., & Houston, T. G. (2012). Global Historical Climatology Network - Daily (GHCN-Daily), Version 3.12. doi:http://doi.org/10.7289/V5D21VHZ

Michailovsky, C. I., McEnnis, S., Berry, P. A. M., Smith, R., & Bauer-Gottwein, P. (2012). River monitoring from satellite radar altimetry in the Zambezi River basin. *Hydrol. Earth Syst. Sci., 16*(7), 2181-2192. doi:10.5194/hess-16-2181-2012

Morlot, T., Perret, C., Favre, A. C., & Jalbert, J. (2014). Dynamic rating curve assessment for hydrometric stations and computation of the associated uncertainties: Quality and station management indicators. *Journal of Hydrology, 517*, 173-186. doi:10.1016/j.jhydrol.2014.05.007

Nash, J. E., & Sutcliffe, J. V. (1970). River flow forecasting through conceptual models part I — A discussion of principles. *Journal of Hydrology, 10*(3), 282-290. doi:https://doi.org/10.1016/0022-1694(70)90255-6

Pelletier, P. M. (1988). Uncertainties in the single determination of river discharge: a literature review. *Canadian journal of civil engineering, 15*(5), 834-850. Retrieved from https://www.scopus.com/inward/record.uri?eid=2-s2.0-0024163837&partnerID=40&md5=7f974b9677db876af486ab1cf405ef00

Pereira-Cardenal, S. J., Riegels, N. D., Berry, P. A. M., Smith, R. G., Yakovlev, A., Siegfried, T. U., & Bauer-Gottwein, P. (2011). Real-time remote sensing driven river basin modeling using radar altimetry. *Hydrol. Earth Syst. Sci., 15*(1), 241-254. doi:10.5194/hess-15-241-2011

Petersen-Øverleir, A. (2006). Modelling stage-discharge relationships affected by hysteresis using the Jones formula and nonlinear regression. *Hydrological Sciences Journal, 51*(3), 365-388. doi:10.1623/hysj.51.3.365

Pushpalatha, R., Perrin, C., Moine, N. L., & Andréassian, V. (2012). A review of efficiency criteria suitable for evaluating low-flow simulations. *Journal of Hydrology, 420-421*, 171-182. doi:https://doi.org/10.1016/j.jhydrol.2011.11.055

Revilla-Romero, B., Beck, H. E., Burek, P., Salamon, P., de Roo, A., & Thielen, J. (2015). Filling the gaps: Calibrating a rainfall-runoff model using satellite-derived surface water extent. *Remote Sensing of Environment, 171*, 118-131. doi:http://dx.doi.org/10.1016/j.rse.2015.10.022

Rey, A., de Koning, D., Rongen, G., Merks, J., van der Meijs, R., & de Vries, S. (2015). Water in the Mara Basin: Pioneer project for the MaMaSe project. *Unpublished MSc project report, Delft University of Technology*.

Ričko, M., Birkett, C. M., Carton, J. A., & Crétaux, J. F. (2012). Intercomparison and validation of continental water level products derived from satellite radar altimetry. *Journal of Applied Remote Sensing, 6*(1). doi:10.1117/1.JRS.6.061710

Savenije, H. H. G. (2010). Topography driven conceptual modelling (FLEX-Topo). *Hydrol. Earth Syst. Sci., 14*, 2681-2692.

Schwatke, C., Dettmering, D., Bosch, W., & Seitz, F. (2015). DAHITI – an innovative approach for estimating water level time series over inland waters using multi-mission satellite altimetry. *Hydrol. Earth Syst. Sci., 19*(10), 4345-4364. doi:10.5194/hess-19-4345-2015

Seibert, J., & Beven, K. J. (2009). Gauging the ungauged basin: how many discharge measurements are needed? *Hydrol. Earth Syst. Sci., 13*(6), 883-892. doi:10.5194/hess-13-883-2009

Seibert, J., & Vis, M. J. P. (2016). How informative are stream level observations in different geographic regions? *Hydrological Processes, 30*(14), 2498-2508. doi:10.1002/hyp.10887

Sellami, H., La Jeunesse, I., Benabdallah, S., & Vanclooster, M. (2013). Parameter and rating curve uncertainty propagation analysis of the SWAT model for two small Mediterranean catchments. *Hydrological Sciences Journal, 58*(8), 1635-1657. doi:10.1080/02626667.2013.837222

Shahin, M. (2002). *Hydrology and Water Resources of Africa* (Vol. 41): Springer Netherlands.

Sikorska, A. E., Scheidegger, A., Banasik, K., & Rieckermann, J. (2013). Considering rating curve uncertainty in water level predictions. *Hydrology and Earth System Sciences, 17*(11), 4415-4427. doi:10.5194/hess-17-4415-2013

Stoop, B. M. (2017). *Morphology of the Mara River: Assessment of the long term morphology and the effect on the riverine physical habitat.* Delft University of Technology.

Sun, W., Ishidaira, H., & Bastola, S. (2012). Calibration of hydrological models in ungauged basins based on satellite radar altimetry observations of river water level. *Hydrological Processes, 26*(23), 3524-3537. doi:10.1002/hyp.8429

Sun, W., Ishidaira, H., Bastola, S., & Yu, J. (2015). Estimating daily time series of streamflow using hydrological model calibrated based on satellite observations of river water surface width: Toward real world applications. *Environmental Research, 139*, 36-45. doi:http://dx.doi.org/10.1016/j.envres.2015.01.002

Thyer, M., Renard, B., Kavetski, D., Kuczera, G., & Clark, M. (2011). Improving hydrological model predictions by incorporating rating curve uncertainty (pp. Proceedings of the 34th IAHR World Congress, 2011: pp.1546-1553). Australia: Engineers Australia.

Tomkins, K. M. (2014). Uncertainty in streamflow rating curves: Methods, controls and consequences. *Hydrological Processes, 28*(3), 464-481. doi:10.1002/hyp.9567

Tourian, M. J., Schwatke, C., & Sneeuw, N. (2017). River discharge estimation at daily resolution from satellite altimetry over an entire river basin. *Journal of Hydrology, 546*, 230-247. doi:https://doi.org/10.1016/j.jhydrol.2017.01.009

U.S. Geological Survey. (2014). Digital Elevation Map. Retrieved from www.earthexplorer.usgs.gov

Vrugt, J. A., Gupta, H. V., Bastidas, L. A., Bouten, W., & Sorooshian, S. (2003). Effective and efficient algorithm for multiobjective optimization of hydrologic models. *Water Resources Research, 39*(8), n/a-n/a. doi:10.1029/2002WR001746

Wang-Erlandsson, L., Bastiaanssen, W. G. M., Gao, H., Jägermeyr, J., Senay, G. B., van Dijk, A. I. J. M., Guerschman, J. P., Keys, P. W., Gordon, L. J., & Savenije, H. H. G. (2016). Global root zone storage capacity from satellite-based evaporation. *Hydrol. Earth Syst. Sci., 20*(4), 1459-1481. doi:10.5194/hess-20-1459-2016

Westerberg, I. K., Guerrero, J. L., Younger, P. M., Beven, K. J., Seibert, J., Halldin, S., Freer, J. E., & Xu, C. Y. (2011). Calibration of hydrological models using flow-duration curves. *Hydrol. Earth Syst. Sci., 15*(7), 2205-2227. doi:10.5194/hess-15-2205-2011

WMO. (2008). Guide to Hydrological Practices; Volume I Hydrology – From Measurement to Hydrological Information.

Yadav, M., Wagener, T., & Gupta, H. (2007). Regionalization of constraints on expected watershed response behavior for improved predictions in ungauged basins. *Advances in Water Resources, 30*(8), 1756-1774. doi:https://doi.org/10.1016/j.advwatres.2007.01.005

Yan, K., Di Baldassarre, G., Solomatine, D. P., & Schumann, G. J. P. (2015). A review of low-cost space-borne data for flood modelling: topography, flood extent and water level. *Hydrological Processes, 29*(15), 3368-3387. doi:10.1002/hyp.10449